Annals of Nuclear Energy 195 (2024) 110143

Contents lists available at ScienceDirect

Annals of Nuclear Energy

journal homepage: www.elsevier.com/locate/anucene

Methods for the radioactive release estimation under DEC-A conditions

Tadas Kaliatka *, Tomas Kačegavičius, Algirdas Kaliatka, Mantas Povilaitis, Andrius Tidikas, Andrius Slavickas

Laboratory of Nuclear Installation Safety, Lithuanian Energy Institute, Breslaujos g. 3, LT-44403 Kaunas, Lithuania

ARTICLE INFO

Keywords:
BWR-4
DEC-A
ASTEC
TRANSURANUS
R2CA

ABSTRACT

After the Fukushima Daiichi Nuclear Power Plant accident, the importance was raised to strengthen the assessment of the safety level of Nuclear Power Plants (NPP) by considering situations more severe than those integrated during the design of the plants. Design Extension Conditions (DEC) term was introduced by IAEA and WENRA. One of the most important subjects in the analysis of these conditions is the evaluation of radiological consequences.

The Reduction of Radiological Accident Consequences (R2CA) collaborative project started in 2019 in the frame of the Horizon-2020 Program of the European Commission. The project addresses a broad scope of LWR designs (Gen II, III and III +) through the analyses of bounding scenarios of Loss Of Coolant Accidents (LOCA) and Steam Generator Tube Rupture (SGTR) transients and explores DBA and DEC-A conditions. The Lithuanian Energy Institute is taking part in this project as well.

The part of work provided in the frame of R2CA project is presented in this article. The generic BWR-4 type reactor with MARK-I containment was analyzed in the case of DEC-A conditions. In this analysis the main thermal hydraulic processes, fission product release and its transport from the broken loop through containment to the environment were investigated. The number of ruptured fuel assemblies is the key parameter determining the fission product release from the core. The methodology which would help more precisely evaluate the number of failed fuel assemblies is presented in this work. The methodology consists of the application of integral severe accident code ASTEC and fuel performance code TRANSURANUS. Analysis using ASTEC code showed the importance of the reactor core nodalisation scheme. Taking iterative calculations, the relative power to which fuel assemblies remain intact at the selected DEC-A condition scenario was obtained. These results were verified with TRANSURANUS code calculations considering the uncertainties of the most relevant parameters. Based on TRANSURANUS calculation results, the ASTEC core nodalisation was improved. Improved ASTEC model nodalisation allowed to calculate more realistic rates of fission products releases from the fuel to the coolant, from the coolant to the containment and as well from the containment to the environment.

1. Introduction

The behaviour of nuclear power plants during Beyond Design Basic Accidents (BDBA) has been widely studied all over the world for several decades. Numerous experimental campaigns (such as PHEBUS (March and Simondi-Teisseire, 2013), CORA (Hagen et al., 1997), QUENCH (Stuckert et al., 2013), CODEX (CODEX), etc.) were provided to investigate the main physical phenomenon occurring in the case of the BDBA. Together with provided experiments, the simulation tools have been developed to consider the complexity of BDBA including thermal-

Abbreviations: ANS, American Nuclear Society; BDBA, Beyond Design Basic Accidents; BWR, Boiling Water reactor; CESAM, Code for European Severe Accident Management; DBA, Design Basic Accidents; DEC, Design Extension Conditions; DW, Containment Drywell; FA, Fuel Assembly; FP7, Seventh Framework Programme; IAEA, International Atomic Energy Agency; IRSN, Institut de Radioprotection et de Sûreté Nucléaire; LEI, Lithuanian Energy Institute; LOCA, Loss Of Coolant Accidents; LOOP, Loss Of Offsite Power; LPCI, Low Pressure Coolant Injection; LWR, Light Water Reactor; NPP, Nuclear Power Plant; PDF, Probability Distribution Function; R2CA, Reduction of Radiological Accident Consequences; RC, Radiological Consequences; SA, Severe Accident; SAM, Severe Accident Management; SGTR, Steam Generator Tube Rupture; TAF, Top of Active Fuel; WENRA, Western European Nuclear Regulators Association; WW, Containment Wetwell.

* Corresponding author.
E-mail addresses: Tadas.Kaliatka@lei.lt (T. Kaliatka), Tomas.Kacegavicius@lei.lt (T. Kačegavičius), Algirdas.Kaliatka@lei.lt (A. Kaliatka), Mantas.Povilaitis@lei.lt (M. Povilaitis), Andrius.Tidikas@lei.lt (A. Tidikas), Andrius.Slavickas@lei.lt (A. Slavickas).

https://doi.org/10.1016/j.anucene.2023.110143
Received 6 June 2023; Received in revised form 11 September 2023; Accepted 18 September 2023
Available online 3 October 2023

Table 1
General information related to ATRIUM fuel assemblies (Fuel, 1997); (Ghasabian et al., 2021).

Framatome ANP, ATRIUM 10A/B	
Assembly geometry	10x10
No of rods per assembly	91
-Water channel	3x3 rod positions
Overall assembly length, mm	4470
Overall assembly width, mm	134
Rod length, mm	4081.4
Rod outside diameter, mm	10.05
Pellet length, mm	10.5
Pellet outside diameter, mm	8.67
Pellet density, g/cm^3	10.55
Average linear fuel rating, kW/m	14.3
Peak linear fuel rating, kW/m	47
Inner cladding pressure, MPa	3
Cladding material	Zy2, LTP2, Fe enhanced Zr liner
Cladding thickness, mm	0.605
Grid material	Zy

hydraulics, thermo-mechanical and chemical processes as well as the possibility of evaluating the fission product releases and transport in the reactor cooling circuit, containment and potentially to the environment. Simulation tools were validated against the provided experimental data. These simulation tools have been currently used for safety analyses, to check the compliance of the safety features of a power plant with the safety requirements and increase the predictability of BDBA progression.

The research and development efforts on the evaluation of Severe Accident (SA) progression and consequences have been strengthened after the Fukushima Daiichi Nuclear Power plant accidents notably under research programs funded by the European Commission through the FP7 and the H2020 frameworks and by OECD/NEA/CSNI. These programmes lead or are targeting to increase the predictability of SA progression, to assess Severe Accident Management (SAM) strategies or to improve mitigation of accident consequences.

The Fukushima Daiichi Nuclear Power Plant accident prompted a comprehensive review of safety analysis approaches, particularly in Europe. As a result, it has become increasingly important to globally strengthen the assessment of Nuclear Power Plant (NPP) safety levels. This includes the consideration of situations that are more severe than those initially integrated into the plant's design. This emphasis on comprehensive safety analysis has become a crucial aspect of NPPs' operations, ensuring that they can withstand extreme scenarios and continue to operate safely. To ensure comprehensive preparedness, it is necessary to consider additional events or combinations of events, and subsequently develop specific provisions to address them. This has been clearly stated through the definition of the so-called Design Extension Conditions (DEC) notably by the IAEA (IAEA, 2016); (Safety Glossary, 2018) and the WENRA (WENRA, 2014. The DEC domain has been split into two different subdomains: the DEC-A for which the prevention of significant core degradation can be achieved and having a higher probability of occurrence than the Severe Accident conditions of the DEC-B (significant core melting). Although the methodologies for the safety evaluation of the DEC-A are different from those used for the Design Basis Accidents (DBA) as the safety margins are supposed to be lower, the models and tools used to analyze bounding scenarios belonging to the DEC-A can be used to verify that the safety margins expected for bounding DBA are sufficiently large.

At the same time, the current practice confirms that the evaluations of radiological consequences for DBA conditions are done using very conservative deterministic assumptions mostly based on decoupled approaches. Moreover, in-line with the European Union directive 2014/87/Euratom of 8 July 2014 (Official Journal of the European Union, 2014), the methodologies used in the past to establish the safety margins of NPP have to be reviewed continuously considering the changes that occurred from the licensing and start times and that include the modifications of the operation conditions (fuel burn-up is an example) and the risks exhibited by the knowledge improvements (e.g. secondary hydriding, high local burn-up and restructured zone, release rate of Cs and I, and others).

The 4-year Reduction of Radiological Accident Consequences (R2CA) collaborative project started in 2019 in the frame of the Horizon-2020 Program of the European Commission. The project brings together 17 partners from 11 countries around the best-estimate evaluations of radiological consequences (RC) from LWR and, in corollary, around proposals for improvements of NPP accident management strategies and safety devices. The project addresses a broad scope of LWR designs (Gen II, III and III +) through the analyses of bounding scenarios of Loss Of Coolant Accidents (LOCA) and Steam Generator Tube Rupture (SGTR) transients and explores DBA and DEC-A conditions. The Lithuanian Energy Institute is taking part in this project as well.

This article presents the part of LEI work provided in the frame of R2CA project. This is an example of consolidating assessments of radioactive releases in the case of DEC-A at BWR-4 reactor accident. Because the number of ruptured fuel assemblies is the key parameter determining the fission product release from the core, the methodology which would help more precisely evaluate the number of failed fuel assemblies is presented in this work. The analysis was carried out in four stages:

1. Initial simulation case. The initial inventory of the fuel was calculated using the SCALE program package and it was set to all calculation cases (Section 2). The model of the generic BWR-4 type reactor with the MARK I containment, which was developed using ASTEC code in the frame of CESAM project (Chatelard et al., 2014a) has been adapted and improved for the LOCA DEC-A condition analysis (Sections 2.1 and 3). The reactor core nodalisation scheme with four concentric rings was developed, distributing the relative power for each ring considering the loading pattern. The performed initial calculations allowed to evaluate roughly the number of fuel assemblies, where fuel claddings failed. This analysis is presented in Section 3.1 in Fig. 10 of the current paper.
2. To verify the accuracy of the ASTEC calculations, a more detailed investigation of the processes in the single fuel rod during the selected accident scenario was conducted using the TRANSURANUS fuel performance code. The analysis revealed a narrow margin between the burst and equivalent stress at the selected relative power, prompting an uncertainty analysis. The following analysis evaluated the cladding stresses, oxidation, fuel pellet and cladding radius changes, and other relevant phenomena. Based on the results, it was concluded that fuel assemblies operating at a relative power of 0.98 will not rupture during the analyzed accident scenario, taking into account the estimated uncertainties. The complete analysis is presented in Section 4 of this paper.
3. Based on TRANSURANUS calculation results, the ASTEC core nodalisation was updated by recalculating the relative power distribution in the fuel assemblies' model in concentric rings of the reactor core. The performed ASTEC analysis, presented in Section 5 of the current paper, allowed the calculation of a realistic number of fuel assemblies with claddings failure.
4. The improved ASTEC model nodalisation facilitated the computation of more realistic rates of fission product release from the fuel into the coolant, from the coolant into the containment, and subsequantly from the containment into the environment, as described in Section 6.

This finally received information on radioactive releases is very important for the further preparation of accident management measures.

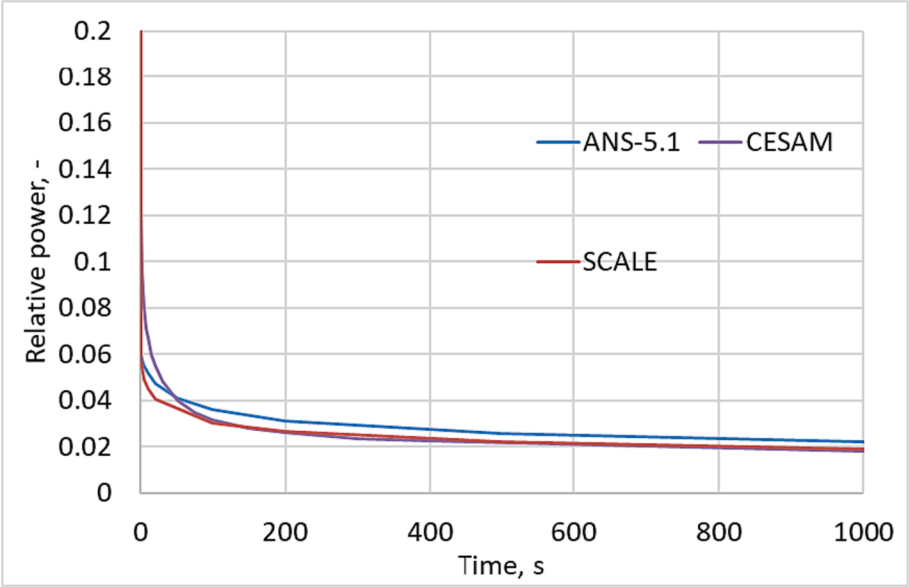

Fig. 1. Relative decay heat power.

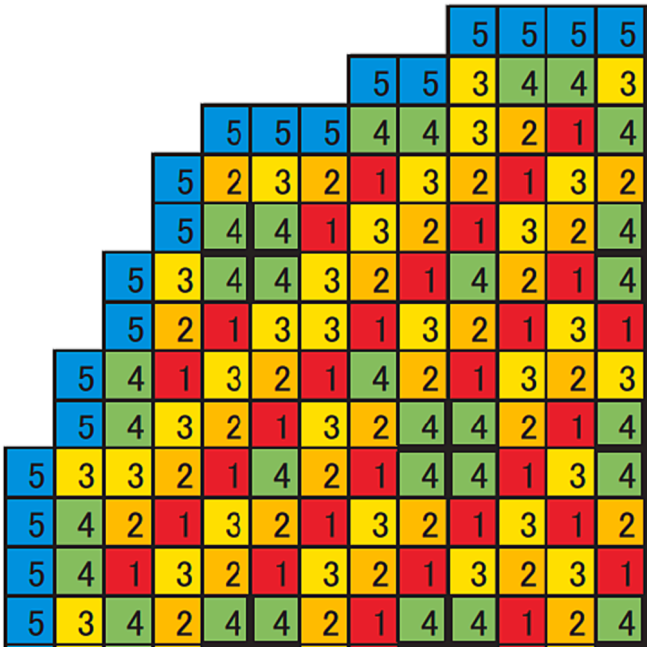

Fig. 2. Fuel assemblies load pattern (quarter of reactor zone) (Keisuke et al., 2012).

2. Generic BWR-4 reactor and main assumptions

The generic Boiling Water Reactor (BWR) of class 4 with Mark I containment (Chatelard et al., 2014a) was selected for the analysis. This type of reactor and containment was constructed in Fukushima Daiichi NPP. This reactor has two recirculation loops and consists of 548 fuel assemblies. The thermal power of the reactor is 2381 MW.

To identify the initial inventory of the fuel, the SCALE 6.2.3 program package was used to perform the neutron transport calculations (Code System and Ornl, tm-2005, 39, 2018). The TRITON/T-NEWT sequence was employed for deterministic neutrons transport and depletion simulations. BWR fuel assembly of ATRIUM-10 design was depleted till it reached the burnup level of 26 GWdays/tonU. The fuel composition at this burnup level was assumed as the initial fuel inventory for the ASTEC model. ATRIUM-10 is the modern 10 × 10 BWR design fuel assembly, with a large internal water channel (Table 1). The numerical model of the assembly was compiled by using data from a Nuclear Energy Agency BWR-MOX benchmark (Oecd, nea, 2003). The benchmark presents the necessary data of geometry and material composition for the compilation of a 2D model.

Decay heat power is a crucial boundary condition, especially for thermal–hydraulic simulations. Decay heat curves are presented in Fig. 1. For the numerical model, it was decided to use the ANS-5.1 decay heat curve (ANS-5.1, 1973). This curve is more conservative in the case of more produced decay heat, in comparison to the data initially utilized in the BWR-4 model developed by the CESAM project (Chatelard et al., 2014a), as well as the decay heat calculations performed using the SCALE code based on the initial inventory provided for ASTEC calculations.

The load pattern for fuel assemblies (Fig. 2) was assumed according to the reference (Keisuke et al., 2012). The assumed load pattern has 5 regions of fuel assemblies grouped by the power history presented in Fig. 3.

Based on to the information given in the reference (Keisuke et al., 2012), the average axial power distribution has been calculated and is presented in Fig. 4. In the numerical model this axial power distribution was assumed for all fuel assemblies in all regions.

2.1. Scenario description

The initiating event of the scenario is a double-ended break of the main recirculation pipe, which occurred when the reactor was operated at full power – 2381 MW. Low Pressure Coolant Injection (LPCI) system was only available in the selected scenario. It was assumed, that LPCI system started at t = 100 s after the accident, when the water level in the core downcomer is above 5.24 m (Top of Active Fuel (TAF)) or pressure in the separator is $\leq 6.9 \times 10^5$ Pa. Such conservative assumptions were used to evaluate the delay of activation due to possible power failures, the combination of Loss Of Offsite Power (LOOP).

The LPCI system injects emergency core cooling water into the recirculation loop discharge piping between the discharge valve and the reactor vessel. A detailed view of the BWR-4 recirculation system is presented in Fig. 5. The recirculation system suction and discharge valves are motor operated valves used to isolate the recirculation pumps

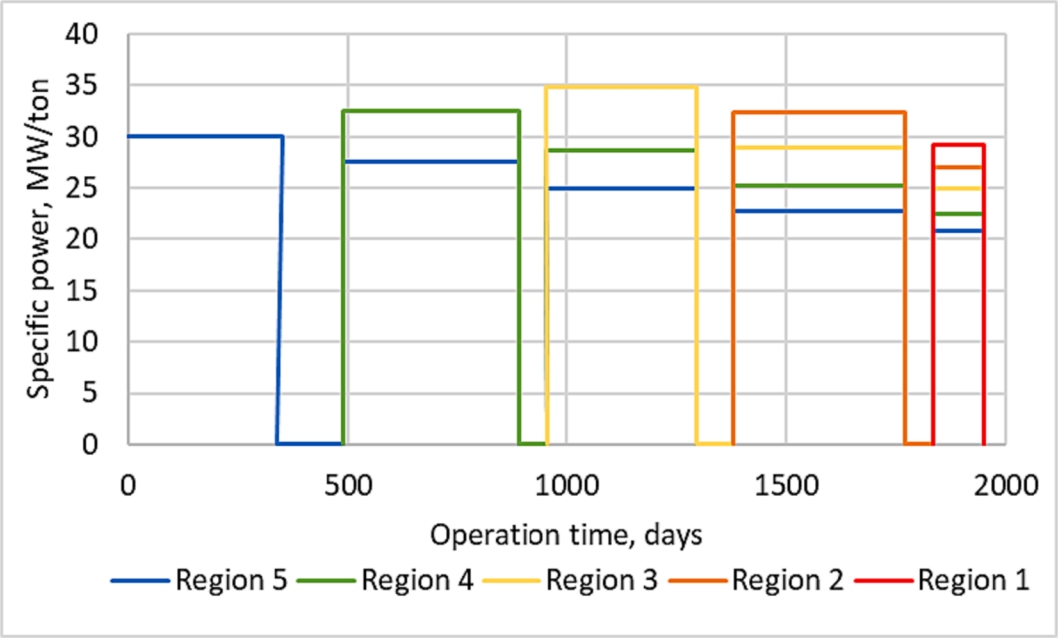

Fig. 3. Power history for each region (Keisuke et al., 2012).

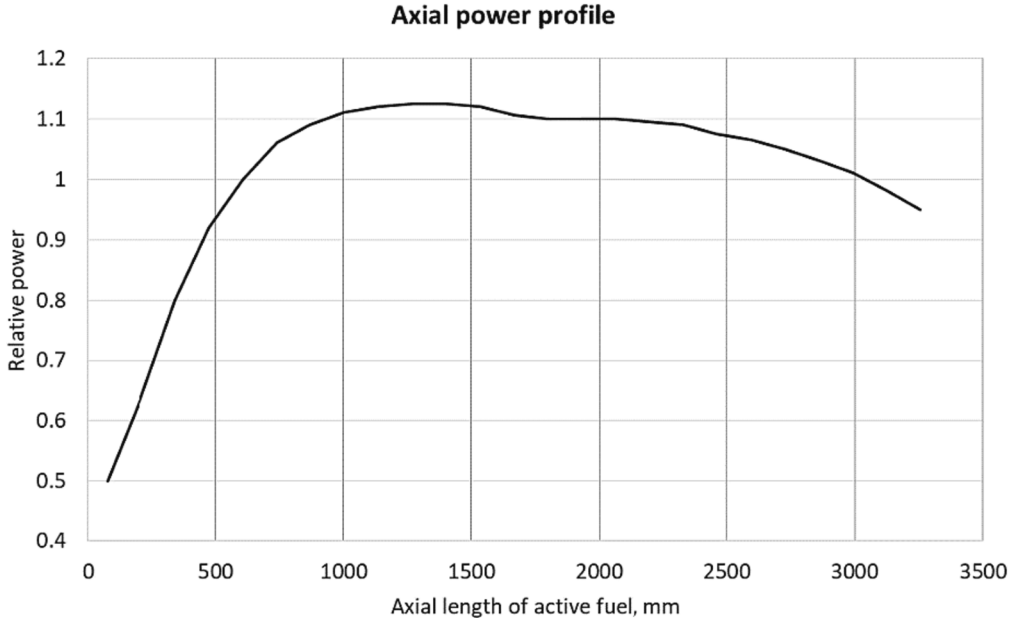

Fig. 4. Axial relative power distribution.

for maintenance. Each valve is individually controlled from the control room by a hand switch. In the calculation, an assumption was made that power plant operators do not take any actions. However, both recirculation loop discharge valves receive an automatic close signal upon a LPCI initiation and low reactor pressure to ensure water introduction into the core (https://www.nrc.gov/docs/ML0230/ML023010606.pdf).

The LPCI injection flow rate varies due to the pressure in the reactor vessel (NUREG-, 1988). The injection flow rate is increasing as the pressure is decreasing (Fig. 6). According to the selected scenario at the time t = 100 s after the accident, when LPCI is available, the pressure in the reactor vessel is ~ 0.4 MPa and later it decreases during the time. For the simulation simplicity, it was decided to use constant a 300 kg/s mass flow rate for the LPCI injection.

In the selected accident scenario, the activation of the containment cooling system was assumed at t = 45 s. This time was considered because within 1 sec from the power outage, auxiliary batteries and compressed air supplies started the emergency diesel generators. Onsite electrical power could be restored ~ 25 s after the outage, but additional time is required to fully start the containment spray. Thus, it was decided to add an additional 20 s. The containment cooling system consists of drywell and wetwell sprinklers. The flow rate of the containment cooling system was assumed 300 kg/s for the simulation.

3. ASTEC model for BWR-4 LOCA scenario

The integral code ASTEC (Accident Source Term Evaluation Code) version V2.1.1.6 was used for the simulations. The Severe Accident (SA) integral code ASTEC (Chailan, et al., 2017), developed by the French

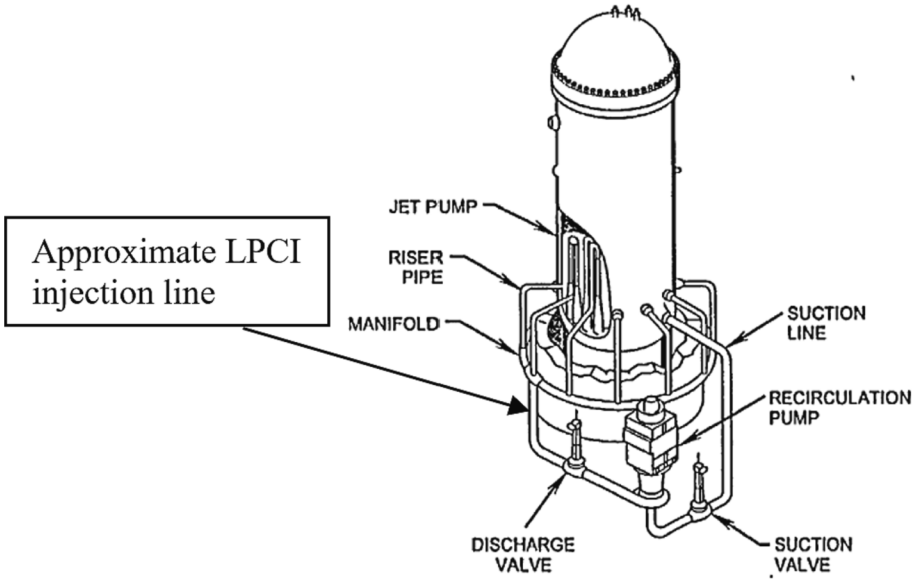

Fig. 5. BWR-4 recirculation system (United States Nuclear Regulatory Commission Technical Training Center).

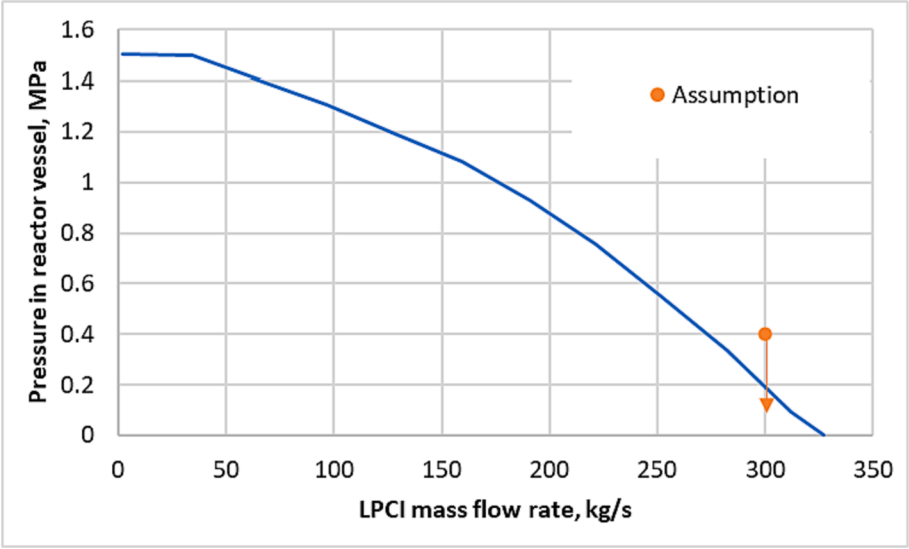

Fig. 6. LPCI flow rate relationship with pressure in the reactor vessel.

Institut de Radioprotection et de Sûreté Nucléaire (IRSN), aims at simulating an entire SA sequence in a nuclear water-cooled reactor from the initiating event up to the release of radioactive elements out of the containment.

The main physical phenomena are validated in more than 20 applications on experiments (validation test-cases), in more than 26 operational test-cases and 16 plant application test-cases. ASTEC code consists of several modules, which are developed for the analysis of separate tasks (Chatelard et al., 2014b). As the basis for the selected BWR-4 LOCA scenario model development in the ASTEC code the model which was developed in the frame of CESAM project (Chatelard et al., 2014a), has been used. This model needed adaptation for the LOCA analysis. Also, model was improved regarding the selected scenario and chosen fuel assembly type. For the developed reactor model the following ASTEC modules were activated to perform the simulations: CESAR, ICARE, CPA, ISODOP, SOPHAEROS, DOSE.

The CESAR module is designated to simulate the two-phase thermal hydraulics of the reactor coolant system during both the front end and the degradation phase (Piar and Treogures, 2009). For this analysis CESAR model was used for the modelling of two recirculation loops see Fig. 7. Recirculation loops represented by volumes: JET_L11, JET_L11A, JET_L12, JET_L13, JET_L21, JET_L22, JET_L23; and junctions between these volumes: JL12JL13, JL22JL23, JL21JL22. Junctions L13_DCE and L23_DCE represent recirculation loops connection to the jet component, while junctions DCE_L11 and DCE_L21 correspond to downcomer connection with recirculation loops. RCP_1 and RCP_2 represent two recirculation pumps to provide water flow rates in the recirculation lines. For the modelling of the main circulation pipe guillotine break, two connections LOCA and LOCA1 connecting the "damaged" recirculation loop and the containment (Drywell zone) are used (Fig. 7). Two connections are needed to simulate possible leakages from both sides of the "damaged" recirculation loop pipe.

Separator, upper head, main steam lines, feedwater lines and top of the downcomer were modeled as well, however they are not presented in the figure. This is because they are crucial for the steady state analysis but become irrelevant for the LOCA scenario as the steam line is closed 5

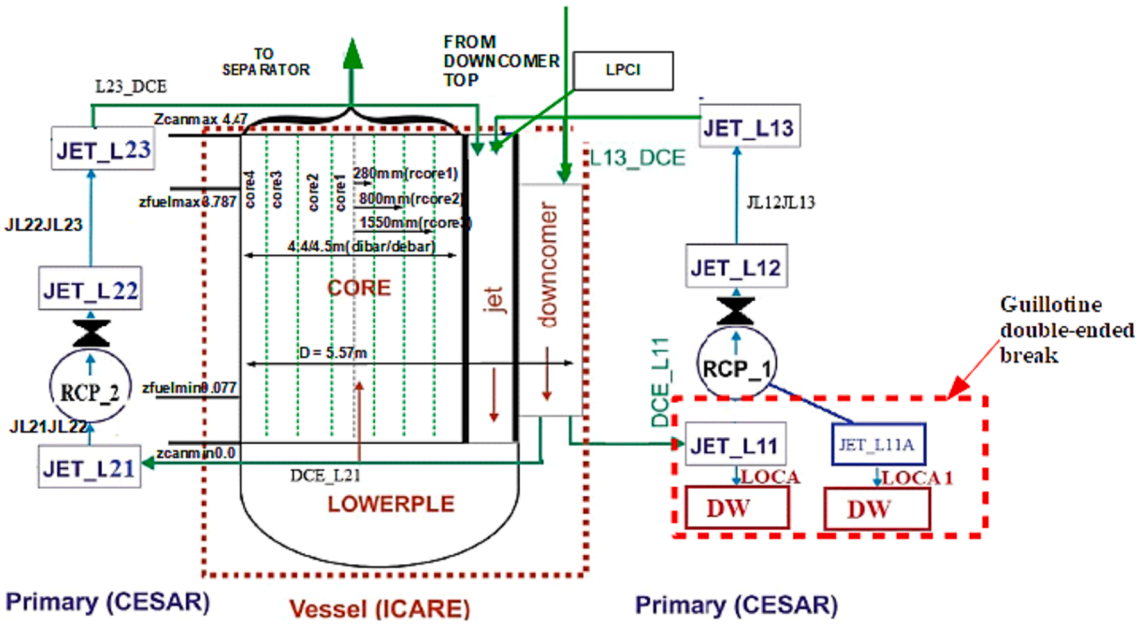

Fig. 7. ASTEC nodalisation scheme of BWR reactor and cooling circuits.

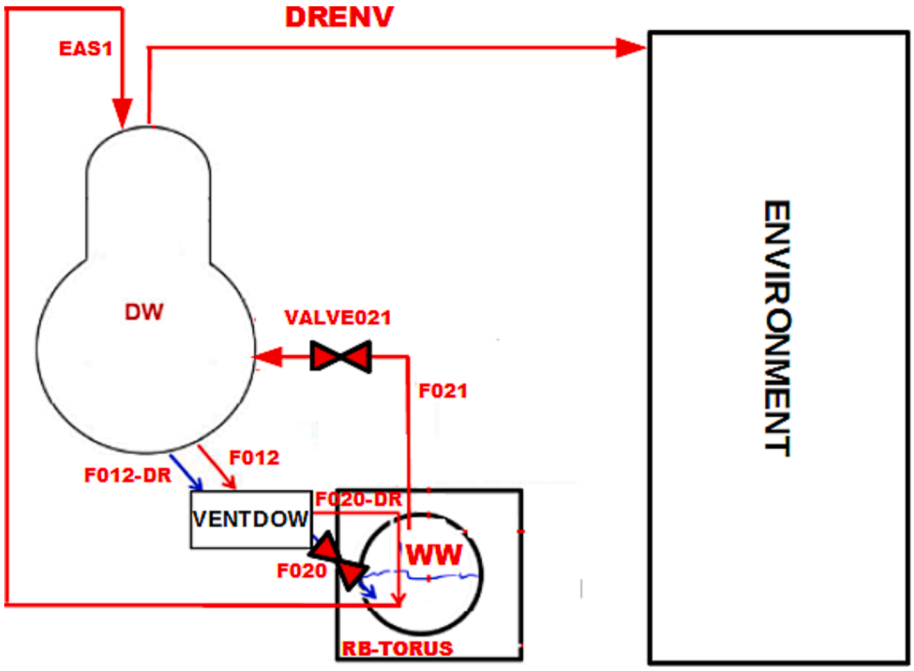

Fig. 8. ASTEC nodalisation scheme of the BWR4-Mark I containment.

s after the accident.

The ICARE module of ASTEC code is used for the in-vessel core degradation simulation. It computes the behavior of in-vessel structures, the formation and the evolution of liquid and solid mixtures and chemical reactions between materials (ASTEC, ICARE). The reactor pressure vessel section is modelled using the ICARE module (Fig. 7). The reactor pressure vessel consists of two parts: a cylindrical part containing the core, downcomer and jet, and a hemispherical part simulating the lower plenum. The vessel made of steel has an inner diameter of 5.57 m and a wall thickness of 130 mm. The reactor core is divided into 4 rings, and 12 meshes in axial direction. Radius or diameters of these rings are shown in Fig. 6. The first ring radius "rcore1" is 0.28 m, the second ring radius "rcore2" is 0.8 m, the third ring radius "rcore3" is 1.55 m and the fourth ring radius "rcore4" is 2.2 m. The total length of reactor core "zcanmax" is 4.316 m (Fig. 6). However, the active core starts 0.077 m from the core bottom "zfuelmin" and finishes at elevation 3.787 m "zfuelmax" which makes 3.71 m active length of the core. Other fuel assembly parameters were selected according to the ATRIUM FA specification presented in Table 1.

BWR-4 containment MARK I was modelled using CPA model (see Fig. 8). The BWR containment model consists of separate zones. For the modelling of mass and energy transport between containment zones, different types of flow connections (junctions) were used. The ASTEC-CPA code distinguishes between atmospheric type junctions (calculating flow rates of gaseous components including carried liquid droplets) and drain junctions (calculating the water flow rate including

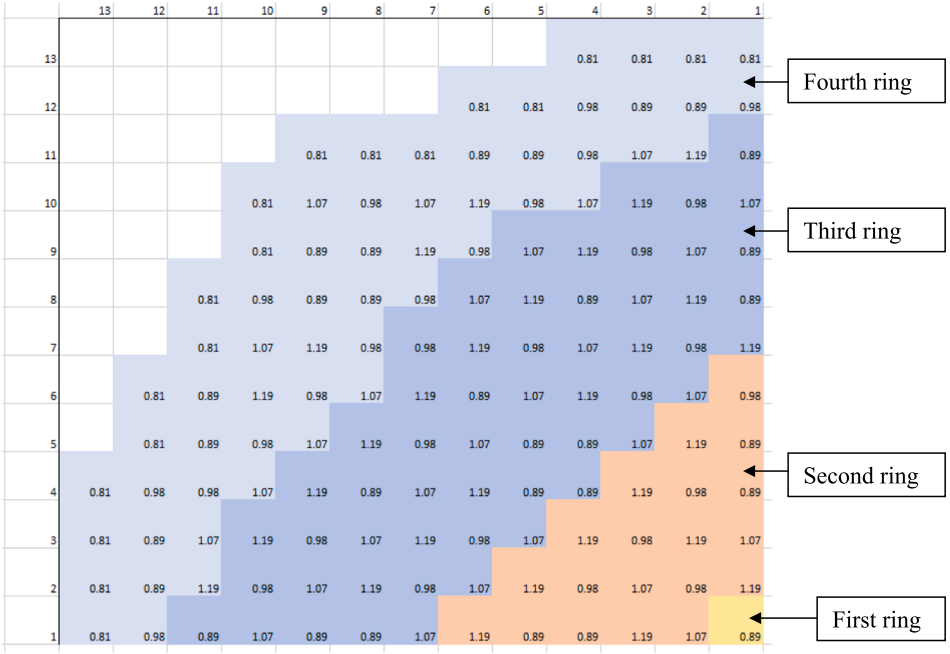

Fig. 9. Initially assumed relative radial power distribution of fuel assemblies in reactor core (quarter of reactor zone).

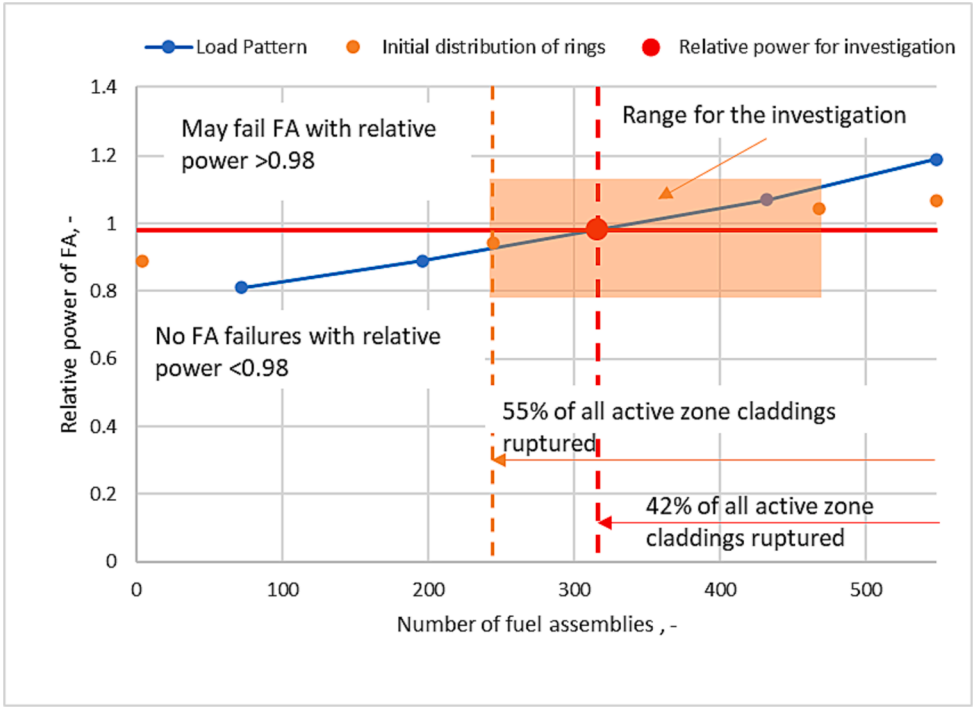

Fig. 10. Relative power vs number of fuel assemblies in the selected loading pattern.

dissolved gas components). The main two volumes, drywell (DW) and wetwell (WW), are connected through vents junctions, drain junction F012-DR and atmospheric type junction F012 from drywell to VENTDOW and drain junction F020-DR and atmospheric type junction F020 from VENTDOW to wetwell. For the vacuum breaker atmospheric type junction F021 with valve from wetwell to drywell is used.

For the modelling of design leakage from the containment to the environment, the connection "DRENV" is used. For the modelling of drywell zone spray system junction EAS1 from WW to DW was used. Containment cooling systems (spray system) of the WW and DW zones are activated by logic considering temperature (temperature in WW < 370 K) and pressure (<0.65 MPa in WW and > 0.17 MPa in DW).

ASTEC modules SOPHAEROS, ISODOP and DOSE were used for the simulation and analysis of fission product release and its transport from the burst fuel claddings to the reactor cooling system, then from the cooling system break to the containment and from the containment through the design leakages to the environment.

SOPHAEROS (ASTEC, SOPHAEROS) is the module of ASTEC dedicated to the simulation of fission products and structural materials transport phenomena in the reactor, i.e. mainly: aerosol agglomeration,

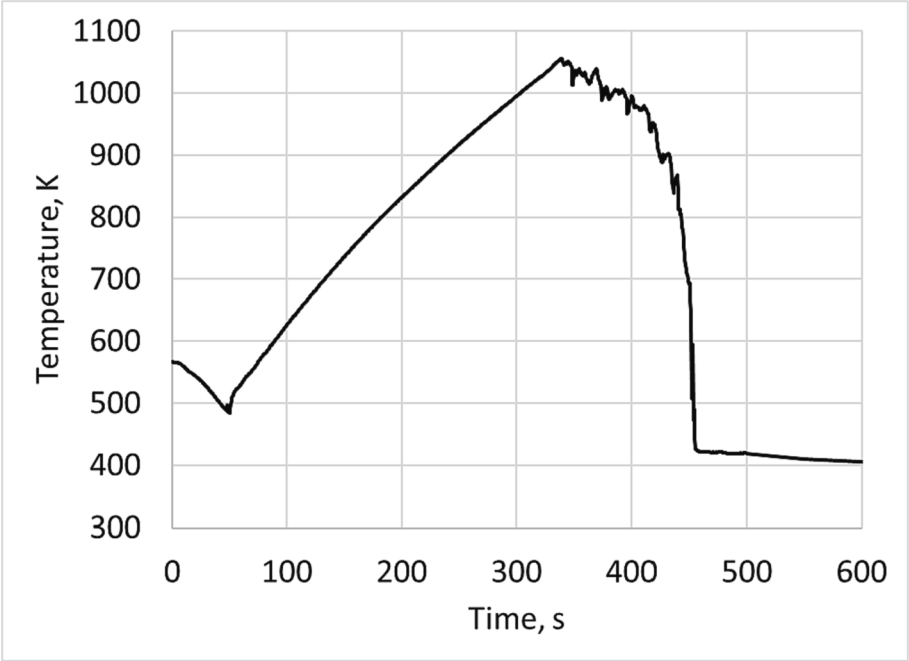

Fig. 11. ASTEC calculation peak cladding temperature in concentric ring with the 0.98 relative power.

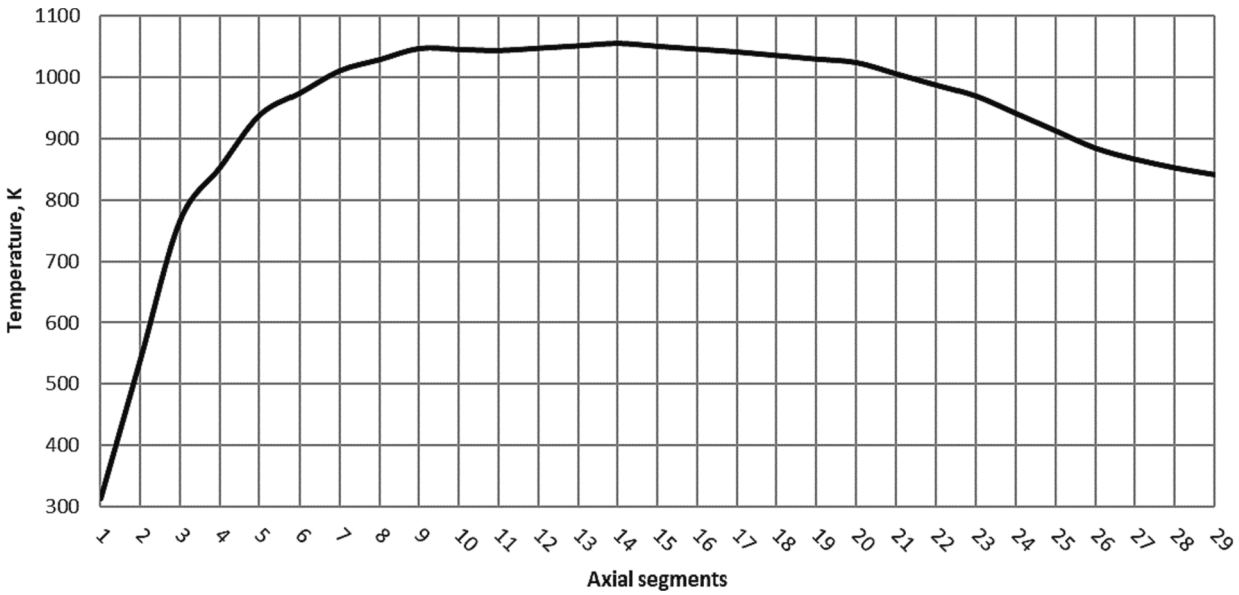

Fig. 12. TRANSURANUS calculated fuel cladding axial temperature profile at peak temperature moment.

deposition and resuspension; vapor phase phenomena (chemistry, nucleation, sorption, condensation); iodine chemistry in containment.

The ISODOP module (ASTEC ISODOP), when coupled with other ASTEC modules that facilitate release, calculates α, β and γ thermal power per unit mass (W/kg), as well as activity (Bq). It also computes the masses (kg) of each element within five domains: core vessel, primary circuit, secondary circuit, containment, and environment, at each time step.

DOSE (DOSE, 2009) is a new ASTEC module designed to estimate the gaseous dose rate in each compartment constituting the containment; it also provides the dose rate onto inner walls of a zone, so two dose rate values are calculated by zone.

3.1. Radial power distribution in ASTEC model

As it was mentioned before, the initial BWR-4 core model developed for the ASTEC code was modelled using 4 concentric rings. The average relative power of each concentric ring was calculated considering core geometry, the load pattern and FA relative power. Fig. 9 presents the relative power of fuel assemblies in the reactor core and the core distribution into 4 concentric rings.

The 1st concentric ring consists of 4 FA with average relative power of 0.89, 2nd ring – 80 FA with relative power of 1.07, 3rd ring – 224 FA with relative power of 1.04 and 4th ring – 240 FA with relative power of 0.94. The performed analysis of LOCA with assumed initial core nodalisation (initial calculation) showed that the fuel assemblies in the second and third concentric rings (relative power 1.066 and 1.043

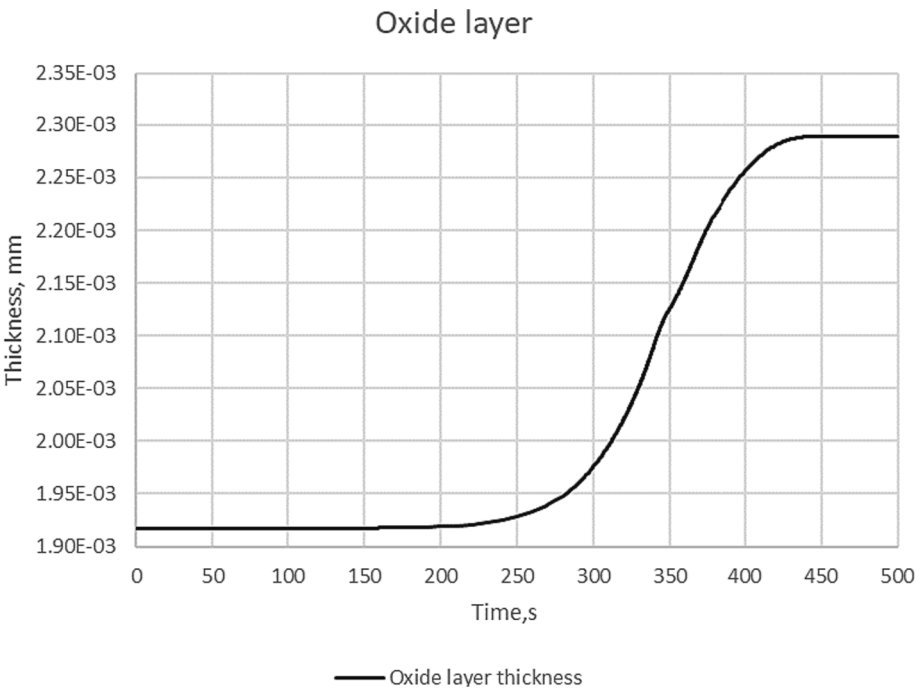

Fig. 13. TRANSURANUS calculated cladding oxide layer thickness (14th segment).

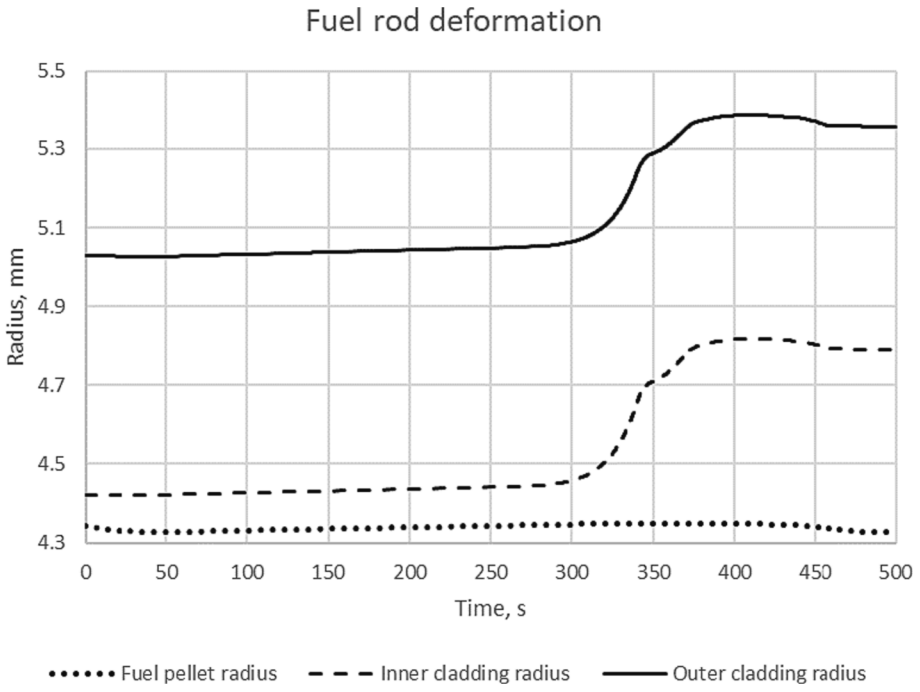

Fig. 14. TRANSURANUS calculated fuel rod deformation (14th segment).

respectively) were ruptured. It corresponds to 55 % of all active zone.

However, this result highly corresponds to the reactor core nodalisation. In this initial nodalisation model, a high step between relative power in the concentric ring 4 (relative power 0.943) and ring 3 (relative power 1.043) is assumed. There are 224 FAs within the relative power range of 0.943–1.043 and in perspective, not all of them could fail (Fig. 10). Thus, a more detailed investigation is needed. Additional calculations were made to investigate at which relative power cladding of fuel rod in FAs could maintain their integrity. After some iterations, it was established that fuel claddings did not burst, if the relative power of FA is 0.98 or less for the given LOCA scenario. However, the limit to the burst is close. More investigations and evaluations are needed to estimate possible uncertainties as the limit is close.

For the verification of the ASTEC calculations and a more detailed investigation of the processes in the single fuel rod with the relative power of 0.98 for the selected accident scenario was provided using TRANSURANUS fuel performance code.

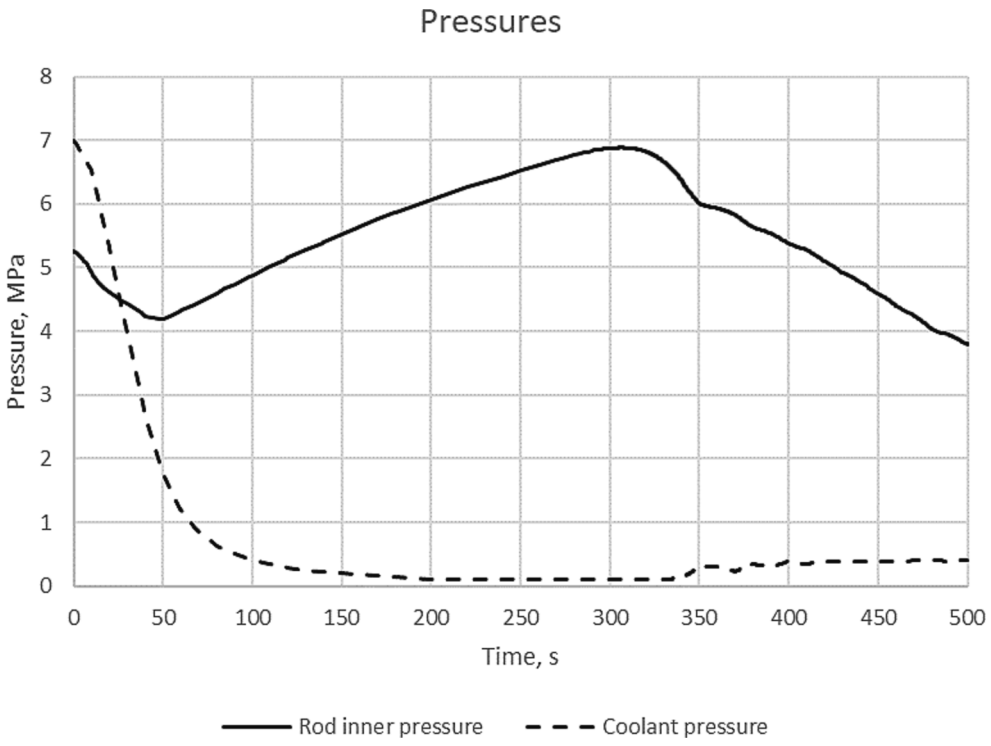

Fig. 15. TRANSURANUS calculated outer and inner pressures in fuel rod.

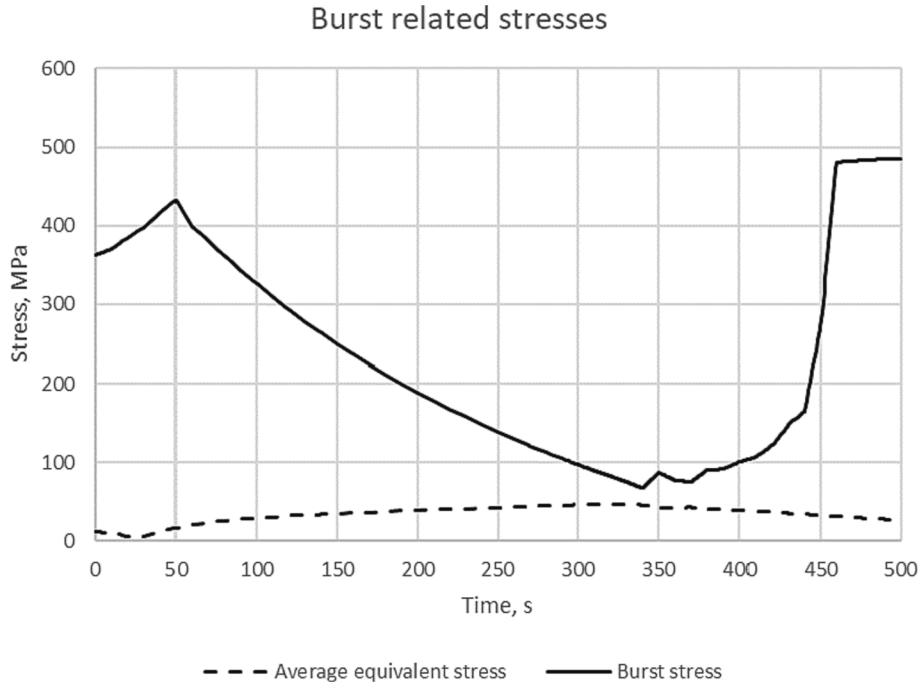

Fig. 16. TRANSURANUS calculated average equivalent stress and burst stress (14th segment).

4. Verification of the ASTEC calculation results with TRANSURANUS code

ASTEC cladding rupture prediction was verified using TRANSURANUS code (TRANSURANUS handbook, 2019), version v1m1j20. For the TRANSURANUS calculations cladding temperature and coolant pressure data were obtained from ASTEC code calculations.

TRANSURANUS is a fuel performance code used to simulate the behaviour of nuclear fuel rods in power reactors under normal and accident conditions. It was developed by the Joint Research Centre (JRC) of the European Commission and is widely used in the nuclear industry (TRANSURANUS handbook, 2019). The code uses a deterministic 1.5D approach to calculate various phenomena that occur in the fuel, such as heat transfer, fission product release, pellet-cladding interaction, and mechanical deformation. It also accounts for the effects of fuel irradiation and burnup, which change the fuel properties over time.

Table 2
Uncertain parameters and selected uncertainty ranges for the uncertainty quantification.

Uncertain parameter	Default value	Uncertainty range	PDF
Pellet radius, mm	4.335	±1%	Normal
Inner cladding radius, mm	4.420	±1%	Distribution
Outer cladding radius, mm	5.025	±1%	
Gap pressure, MPa	3.000	±2%	
Outer pressure, MPa	According to ASTEC calculations	±1%	

For LOCA case, outer cladding temperatures are prescribed by setting the infinitely large heat transfer coefficient from fuel cladding to coolant and assigning previously calculated cladding temperatures.

The BWR fuel rod model was prepared in accordance with the data presented in Table 1. At the start of calculation, the plenum contains helium gas with a pressure equal to 3 MPa. Fuel pellets are made of Uranium Oxide with 3.987 % U^{235} enrichment. This value corresponds to the average enrichment between all rod fuels in BWR ATRIUM-10 design. For cladding material, Zirconium is considered.

URGAS-model is used for fission gas release. An empirical model of fuel pellet densification is used. Visco-elastic treatment of creep in the fuel and explicit treatment of creep in the cladding are assumed. Oxygen redistribution in fuel pellet is not considered. An interaction layer between fuel and cladding is considered in the gap conductance model. Relocation volume is treated as a free volume. Surface boiling is assumed. Grain growth model of Ainscough and Olsen is considered (Ainscough et al., 1973). The Hydrogen content is not considered. No stress dependent fission gas release and swelling model is considered. 0.001 mm of oxide layer is considered at the start of irradiation.

Power history of region 3 as presented in Fig. 3 was considered for the irradiation scenario (prehistory) of analysed fuel rod. It lasts for roughly 1000 days and has three break periods. During this phase, an average linear power equal to 14.3 kW/m is assumed. Neutron flux was calculated from the derived relationship between neutron yield and linear heat rate from the previous calculations and it stands at $6 \bullet 10^{12}$ neutrons per kW/m. Prehistory provides some cumulative strain such as creep strain that furthers influence the rupture possibility in the cladding.

Fuel rod is divided into 29 equal axial segments with a specific power distribution seen in Fig. 4 as the axial power profile. For further analysis, 14th segment will be used as a point of reference as it contains the highest temperature in the observed calculation data.

The TRANSURANUS calculation results did not indicate a fuel rod cladding rupture. There are 4 cladding failure criteria modes in TRANSURANUS code: 1) Overstress 2) Stress/Strain 3) Plastic instability 4) Combined criteria. First two criteria correspond to the material properties while the 3rd criteria can be inputted as an arbitrary value for the effective strain limit. All failure criteria modes were investigated. For the plastic instability criteria default values were used corresponding to the threshold level of effective creep rate at 100 h^{-1} and the effective creep at 2 %.

The fuel rod with the relative power of 0.98 was selected for the analysis using the TRANSURANUS code. Cladding temperatures were obtained from the ASTEC code calculations Fig. 11.

In Fig. 12 the TRANSURANUS calculated cladding axial temperature profile, based on axial relative power distribution (Fig. 4), is presented at the time period (~330 s) when temperature reaches the peak cladding temperature of ~ 1055 K.

TRANSURANUS outer cladding oxide layer thickness, fuel rod deformation during LOCA, average equivalent stress and burst stress, inner (in the gap between fuel pellets and cladding) and outer (coolant around fuel rod) pressures for the 14th axial segment are presented in Fig. 13, Fig. 14, Fig. 15, and Fig. 16.

TRANSURANUS code was used for a more detailed analysis of the processes in fuel behaviour during LOCA in the DEC-A conditions considering using ASTEC code calculated fuel cladding temperatures for FA results with the concentric ring at relative power of 0.98. The

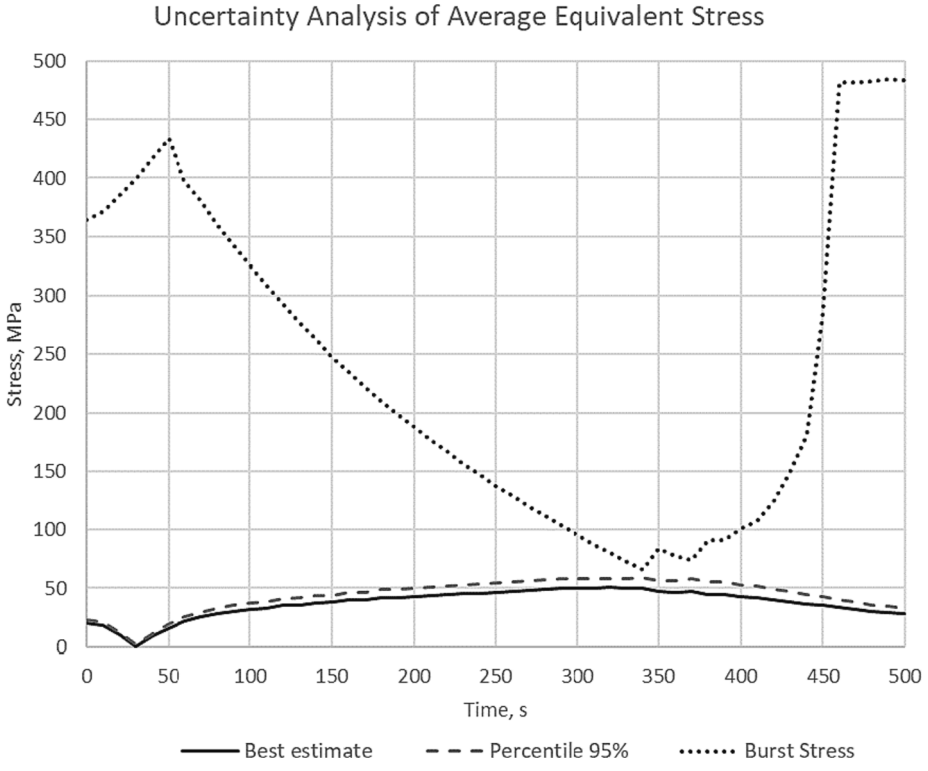

Fig. 17. TRANSURANUS calculated best-estimate and 95% precentile average equivalent stresses with burst stress in cladding (14th segment).

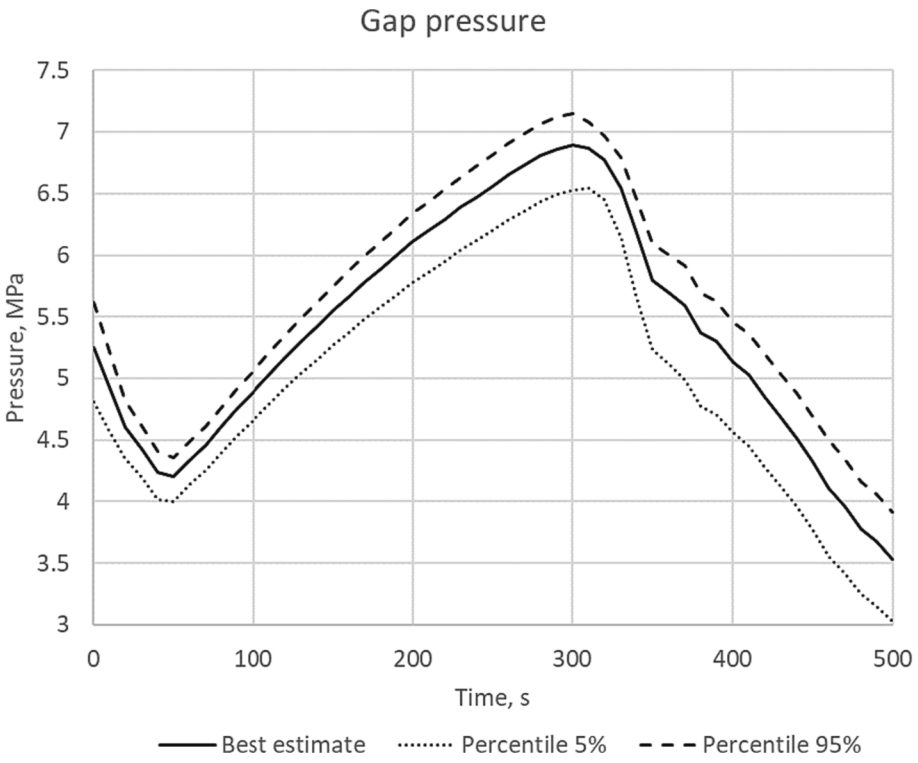

Fig. 18. TRANSURANUS calculated gap pressure (14th segment).

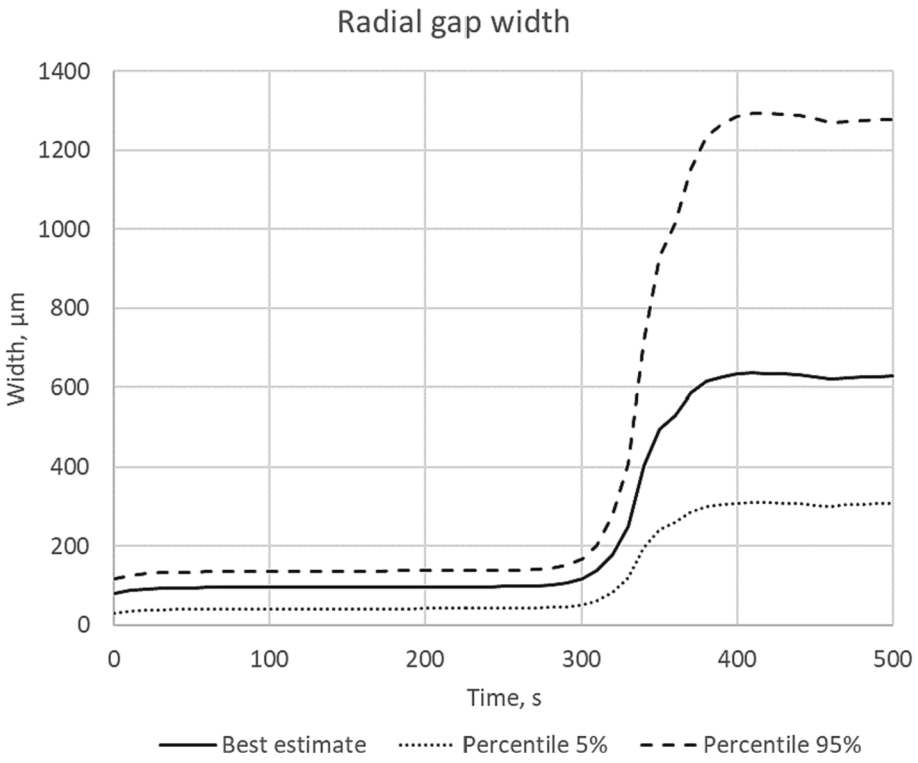

Fig. 19. TRANSURANUS calculated gap width (14th segment).

calculation results did not indicate cladding rupture, corroborating the findings from the ASTEC calculations. Fig. 16 presents the average equivalent stress, representing the forces acting on the cladding, and burst stress, corresponding to the cladding's capacity to withstand bursting. The obtained margin between the average equivalent stress and the burst limit was only ~ 10 MPa and might fall within the range of uncertainties. Thus, it was decided to conduct uncertainty quantification of TRANSURANUS calculation results, as outlined in Section 4.1.

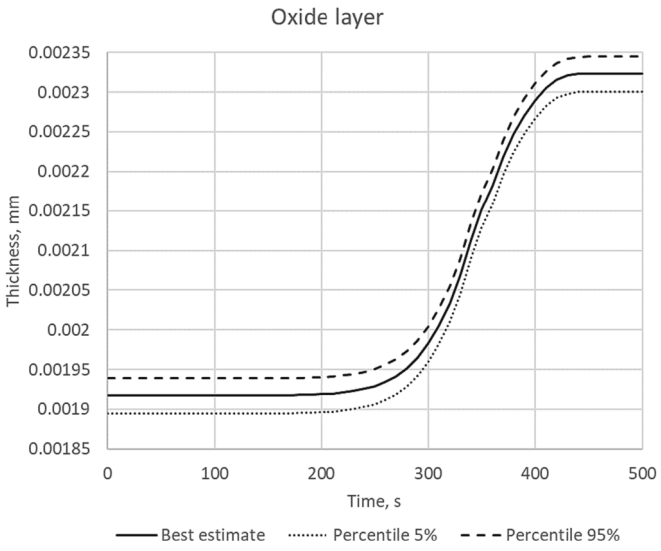

Fig. 20. TRANSURANUS calculated outer oxide layer (14th segment).

Table 3
Relative power distribution through the concentric rings.

	Initial model		Updated model	
Ring	Number of FA	Relative power	Number of FA	Relative power
1	4	0.89	4	0.89
2	80	1.07	72	0.93
3	224	1.04	232	1.13
4	240	0.94	240	0.9
Total	548	Average: 1.0011	548	Average: 1.0012

4.1. Uncertainty quantification for the TRANSURANUS calculation results

As it is presented in Fig. 16 the distance between burst and equivalent stress is very narrow at the time ~ 340 s after the beginning of the LOCA accident. Therefore, it was decided to perform the uncertainty analysis for the TRANSURANUS calculation results to make sure that even with uncertainties bound claddings of the fuel with 0.98 relative power will be intact.

Conservative rupture parameters are being considered as presented in other cases. Five parameters were considered for uncertainty quantification. Uncertain parameters and selected uncertainty ranges for the uncertainty quantification are presented in Table 2. Uncertainty ranges and probability distribution function (PDF) were selected according to the previously provided work in references (Kaliatka et al., 2016; Marao et al., 2013; Kaliatka et al., 2009) and engineering judgment, after the separate sensitivity analysis.

TRANSURANUS code has its in-build Uncertainty and Sensitivity tool (Soti et al., 2018). For the uncertainty analysis, 100 calculations were performed. Results of the uncertainty analysis are presented in Fig. 17–Fig. 20. All presented figures show the results obtained at the 14th axial segment of TRANSURANUS fuel model.

As it is presented in Fig. 17 the average equivalent stress varies in the range of up to ~ 60 MPa (Percentile 95 %), still below the burst stress.

Table 4
Comparison of the results of the main parameters at the steady state calculation.

Main parameters	LEI ASTEC V2.1.1.6	Fukushima Unit 2 (TEPCO)	CESAM ASTEC V2.1.1 (Wang and Muscher, 2018)	KIT ASTEC V2.1rev3 (Vela et al., 2017)
Core thermal power, MW	2381	2381	2381	2381
Total feedwater mass flow rate, kg/s	1256.8	1233.3	1256	1256.26
Total steam line mass flow rate, kg/s	1256.8	1233.3	1253.5	1253.63
Pressure in separator (MPa)	6.97	6.9	6.97	6.97
Feedwater temperature (K)	481.15	488.7	480.1	480.16
Main steam line temperature (K)	558.7	559.2	558.7	558.62
Water recirculation factor	6.5		6.5	6.5

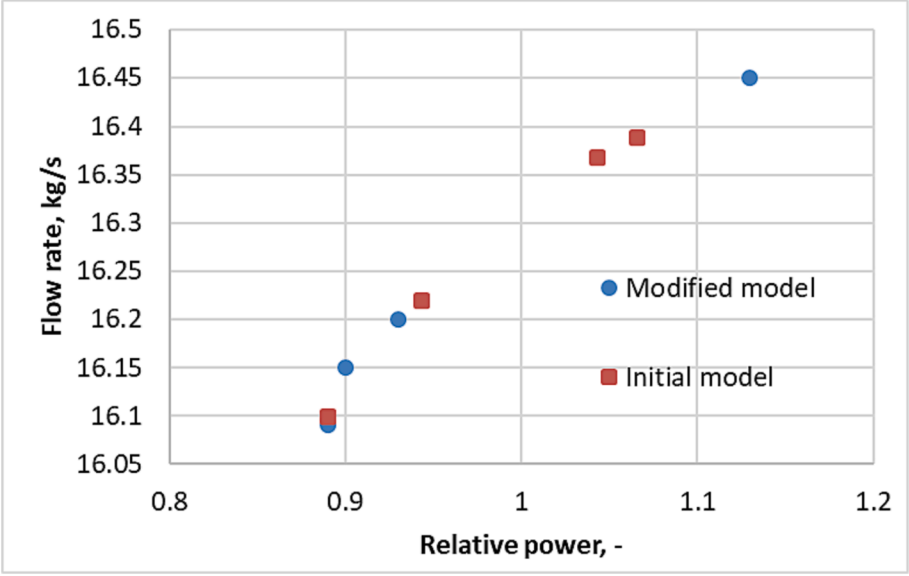

Fig. 21. Coolant flow rate versus relative power of rings.

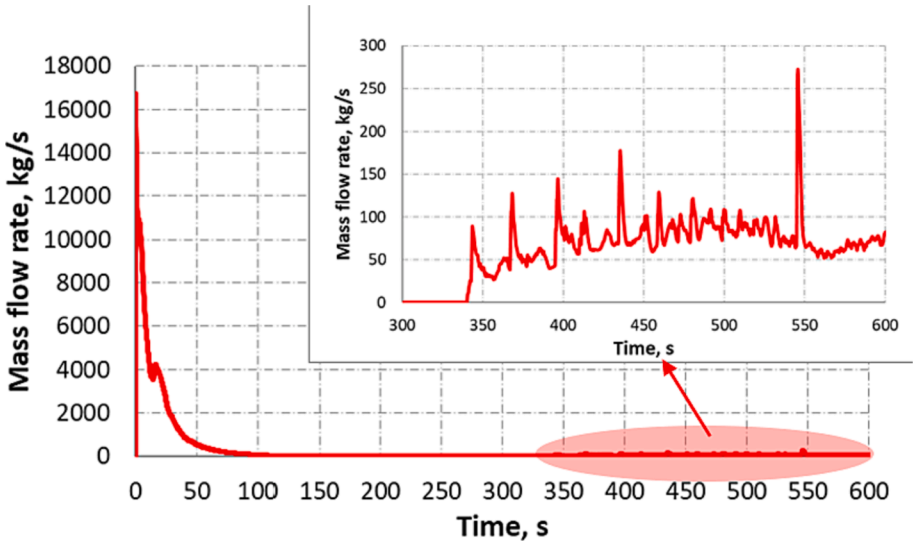

Fig. 22. The mass flow rate through the break (Kaliatka et al., 2022).

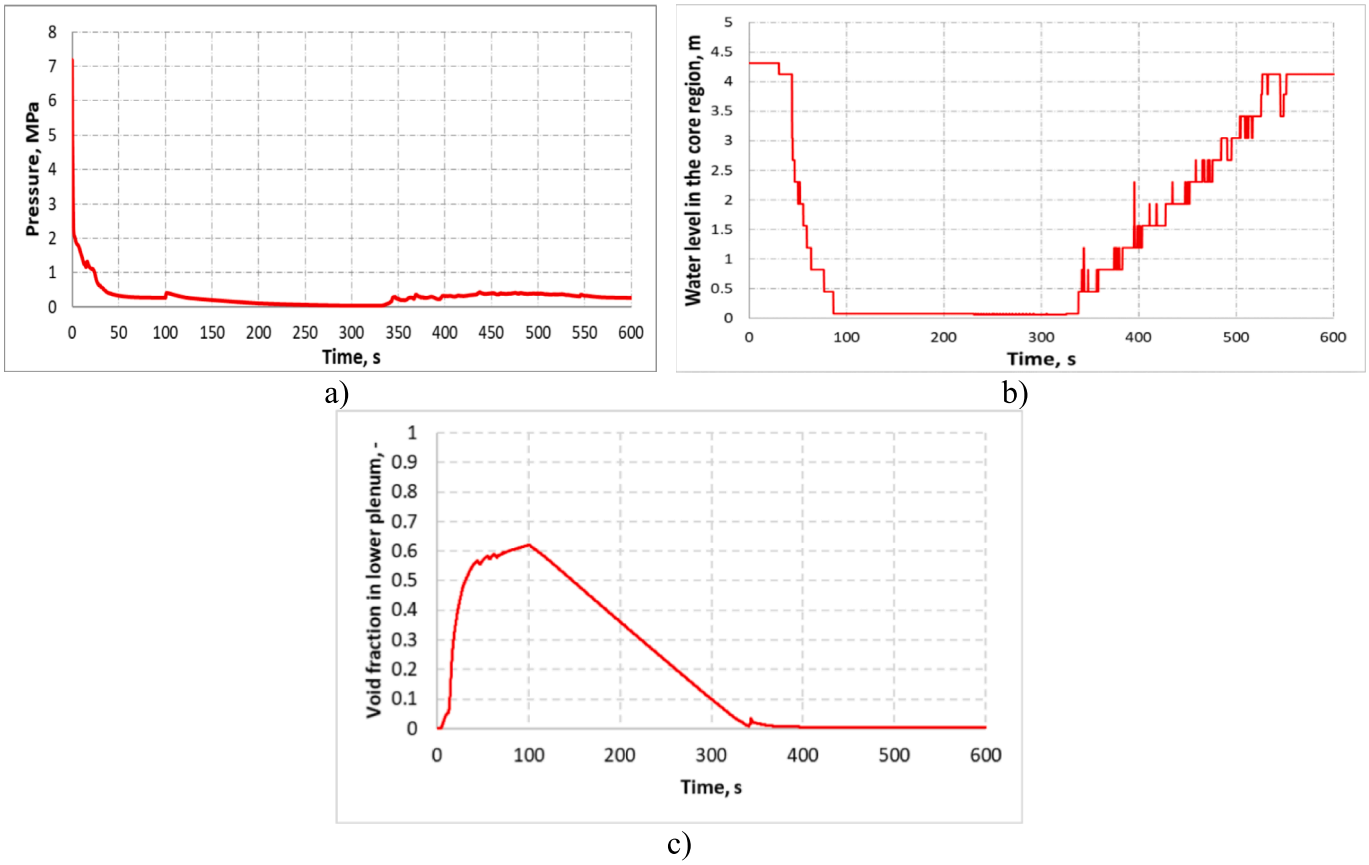

Fig. 23. Calculation results: a) Pressure in the broken recirculation loop; b) Collapsed water level in the core region, from the bottom; c) Void fraction in the lower plenum (Kaliatka et al., 2022).

the calculated burst stress did not show any significant uncertainty since it is entirely dependent on the cladding temperature which has fixed values according to the ASTEC calculations (Fig. 11).

Fig. 18 and Fig. 19 present the pressure evolution in the gap between fuel pellet and cladding and the gap width changes at the 14th segment. Especially high variations are observed in the gap width at 300 s after the transient initiation. The minimum gap width was ~ 200 μm, while the maximum value reaches ~ 1600 μm. The outer oxide layer at the 14th segment is presented in Fig. 20. Discrepancies in the calculation results are uniform during the whole presented calculation period.

5. Comparison of the ASTEC calculation results of initial and updated models

Considering the above-mentioned conclusion that even considering the uncertainties fuel claddings with the 0.98 relative power will be

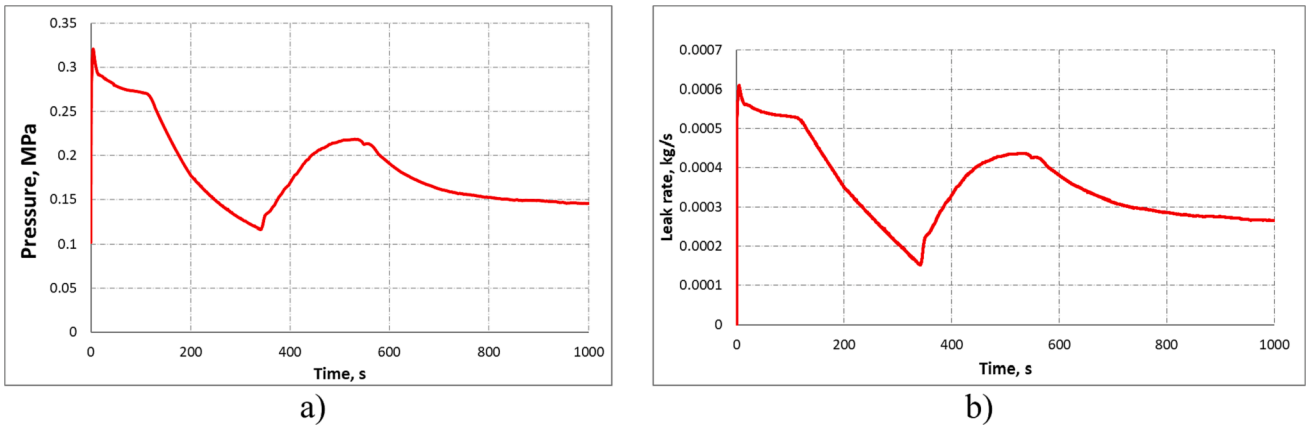

Fig. 24. Calculation results: a) pressure in the containment; b) leak rate from the containment to environment (Kaliatka et al., 2022).

Table 5
Number of failed fuel rods, time, and elevation of failure.

		Number of the failed fuel assemblies	Cladding failure time	Cladding failure elevation from the active fuel bottom
Initial model	Failure of the ring with relative power 1.07	80	358 s	Between 1.932 m and 2.303 *m*
	Failure of the ring with relative power 1.04	224	419 s	Between 1.932 m and 2.303 *m*
	Total:	304		
Updated core model	Failure of the ring with relative power 1.13	232	415 s	Between 1.932 m and 2.303 *m*

intact - the ASTEC core nodalisation model was modified (updated) in order to be more precise in evaluating radiological consequences. According to the assumed load pattern it was decided to collect all FA which potentially could have failures (relative power above 0.98) into one concentric ring. Differences with respect to the initial model are presented in Table 3.

Due to the modification of the core nodalisation (difference in FA number and the relative power) the flow rate through the channels at steady state (operational) conditions changed. Therefore, the flow rate through the channels was tuned (by changing form losses through the core) to be in line with the initial model and according to the general configuration of the BWR type reactors.

Fig. 21 represents steady-state coolant flow rates versus relative powers of rings for the initial and modified (updated) models. The flow rate versus relative power is congruent in one line. This result shows adequate steady-state behaviour of the updated model and allows further LOCA transient simulations.

The results of the steady-state calculation, before the start of the transient, with the main parameters are presented in Table 4. Steady-state calculation is presented together with the measurements from Fukushima Daiichi Unit 2 (TEPCO) and other calculation results provided by different users (calculation results presented in CESAM project (Vela et al., 2017) and calculations presented by KIT (Wang and Muscher, 2018). Calculation results are close to Fukushima Daiichi Unit 2 data and calculation results achieved by other code users.

Thermal hydraulic parameters calculated with modified (updated) active core nodalisation showed almost identical results compared to the results obtained with the initial model (section 3). There are only some small differences that are not significant. These small differences can be caused mainly by the calculation time step variations and approximations in the ASTEC code itself.

The modifications presented in the updated model led to differences in the fuel rods and the release of fission products. The influence of the modifications on the thermal–hydraulic transient of the accident (coolant releases and pressure evolutions) is insignificant. Therefore, in the following discussion only the thermal–hydraulic transient obtained with the updated model is presented, while fuel rod failures and fission

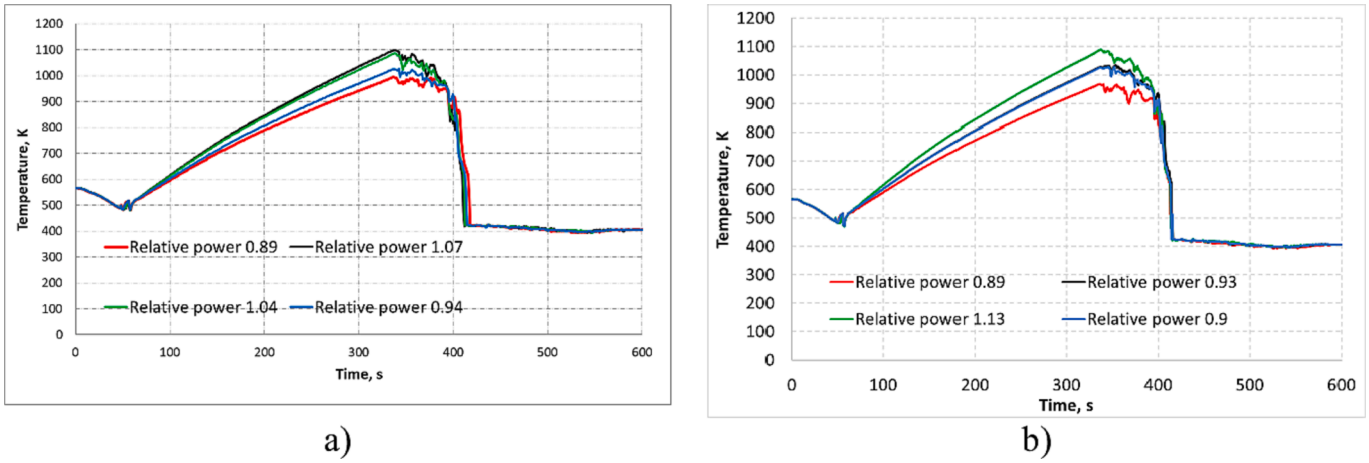

Fig. 25. Peak cladding temperature in different rings of fuel assemblies: a) results from initial model; b) results with updated core model.

Table 6
Release fraction of 5 most important elements (Cs, I, Xe, Kr, Te) from the bundle and through break at the 2000 s calculation time form the start of the transient.

		Fraction		Difference between models, %
		Initial model	Updated model	
Release from fuel	Cs	2.91E-02	2.36E-2	18.8
	I	9.83E-03	8.04E-03	18.2
	Kr	1.74E-2	1.42E-02	18.6
	Xe	1.74E-2	1.42E-02	18.6
	Te	6.05E-05	4.73E-05	21.8
Release through break	Cs	2.67E-02	2.22E-02	16.9
	I	9.82E-03	7.56E-03	23.0
	Kr	1.73E-02	1.41E-02	18.7
	Xe	1.74E-02	1.41E-02	18.7
	Te	5.56E-05	4.42E-05	20.4
Release to environment	Cs	1.29E-08	1.4E-08	8.0
	I	4.39E-09	4.75E-09	8.1
	Kr	1.41E-4	1.12E-4	20.1
	Xe	1.41E-4	1.12E-4	20.0
	Te	2.79E-11	2.81E-11	0.7

product behaviour obtained with both models are compared.

The mass flow rate through the main recirculation pipe break is presented in Fig. 22. During the first seconds after the accident mass flow rate reaches ~ 16000 kg/s, but it sharply decreases and after 120 s mass flow is close to 0 kg/s. This situation occurs due to the pressure (Fig. 23a) and water inventory (Fig. 23b) loss in the recirculation loop and pressure increase in the containment caused by the break. The water level in the core region and void fraction in the lower plenum (Fig. 23b and c) indicate the reactor water inventory loss. The obtained results show that the lower plenum contains boiling water. Steam from the lower plenum rise to the reactor core and fuel assemblies are cooled by steam. Steam has much lower heat transfer coefficient compared to water and this causes the heat up of the fuel assemblies. According to the selected scenario, LPCI system is activated 100 s after the start of the accident. Water injection using this safety system terminates the further increase of the void fraction in the lower plenum. It was assumed constant 300 kg/s flow rate of LPCI system until the core region is filled. Further LPCI system work is restricted to maintain the water level in the core region.

The mass flow rate through the break increases again when the water

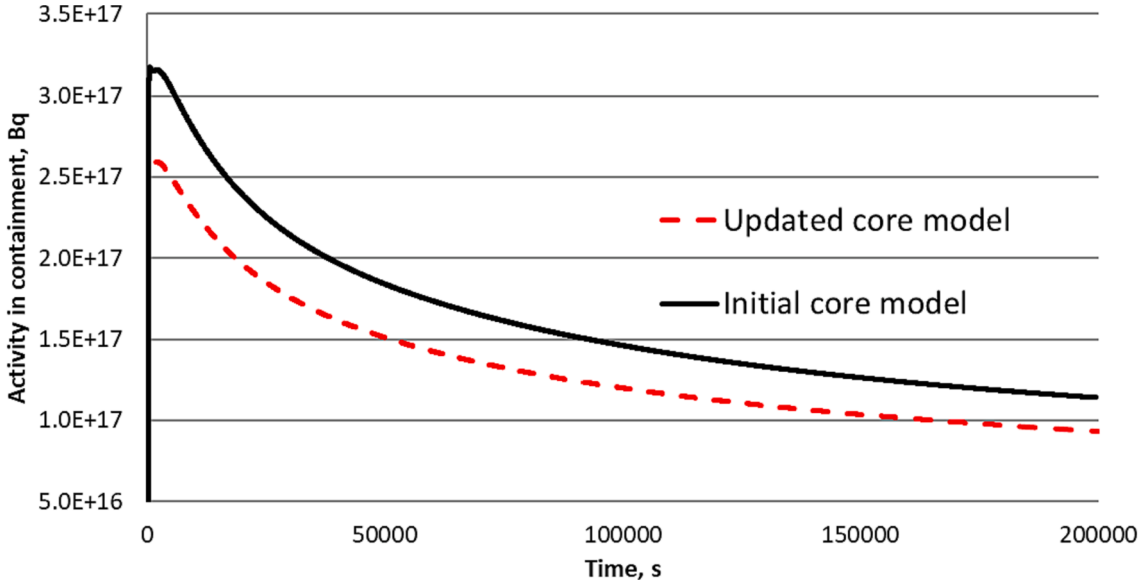

Fig. 26. Comparison of activity in the containment.

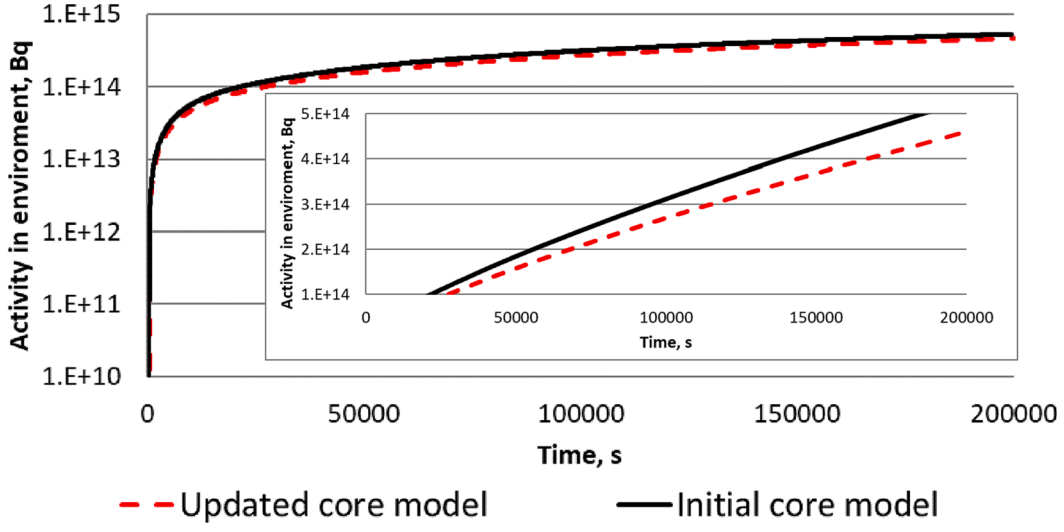

Fig. 27. Comparison of activity in the environment.

injected by LPCI system reaches the lower part of the active fuel after 300 s (Fig. 22, Fig. 23b, c). Cold injected water contacts with hot surfaces in the bottom of the core region – the amount of generated steam is increased, which leads to the pressure increase in the recirculation loop (Fig. 23a). Following the pressure increase, the release through the break also slightly increases (Fig. 21).

During the first seconds of the accident, due to the release of steam-water through the break, the pressure in the containment is increasing above 0.3 MPa (Fig. 24a). The containment spray system activates 45 s after the break, and it helps to decrease the pressure to a slightly higher than atmospheric. However, when the core is re-filled by the LPCI system, steam is generated, and pressure in the containment increases again and only after 1000 s stabilizes to ~ 0.15 MPa pressure. Containment design leakage is 0.5 % of vol/day. However, with an increase of pressure in the containment, the mass flow rate from the containment to the environment is also increasing (Fig. 24 b)). The maximum obtained flow rate from the containment to the environment is 0.0006 kg/s, after the stabilization of the pressure in containment (1000 s) flow rate stabilizes at ~ 0.00025 kg/s.

The comparison of the number of failed fuel rods, time and elevation of failure is presented in Table 5. The initial model showed failures in the two rings whose relative power were 1.066 and 1.043 respectively. The updated core model was based on the redistribution of FAs based on the relative power higher or lower to 0.98. In this case, all FAs which have higher relative power than 0.98 were simulated in one concentric ring (in total 232 FA with an average of 1.13 relative power). Simulation results showed the failure of this ring. Other rings whose relative power was lower than 0.98 remain intact. This situation is discussed in Fig. 10.

Fig. 25 shows peak cladding temperatures of different fuel assemblies rings (with different relative power) achieved using both calculation models. Results obtained from the initial model showed the maximum temperature of ~ 1100 K in two rings whose relative power was 1.07 and 1.04. With the updated model only one ring with the relative power of 1.13 shows the maximum temperature of ~ 1110 K, while temperatures of other rings reach maximum values below 1100 K.

The lower number of failed fuel assemblies obtained with the updated model has a positive impact on the severity of the accident regarding released radioactive fission products, as is illustrated by Table 6.

The table shows that overestimating the number of failed fuel rods in the original model simulations leads to incorrect prediction of radioactive releases by at least around 20 %.

Lower releases consequentially resulted in lower activities in the containment and environment, as is shown by Fig. 26 and Fig. 27. Comparing the calculation results of the initial and the updated core models ~ 18 % activity decrease at the 200000 s time from the start of the transient in the containment is obtained.

Activity in the environment, presented in Fig. 27, is the most important parameter used for the evaluation of the radiological consequences. In the presented simulations only the containment design leakages were considered as environmental release pathways. After ~ 1000 s pressure in the containment stabilizes together with the leak rate from the containment to the environment. This gives the linear increase of the activity in the environment after 1000 s since in the scenario there were no measures to reduce the containment activity foreseen. Comparing the calculation results of the initial and updated core models ~ 13 % activity decrease at the 200000 s time from the start of the transient is observed.

6. Summary and conclusions

The generic BWR-4 model for the ASTEC code was adapted and improved to analyze the main thermal hydraulic processes, fission product release and its transport from the broken loop to the containment and to the environment. For the analysis, the LOCA transient scenario corresponding to DEC-A conditions was selected.

The initial ASTEC core nodalisation scheme consisted of 4 concentric rings for which relative power was calculated considering the loading pattern and the geometrical distribution of rings. The initial core nodalisation model results showed that during analyzed LOCA transient fuel assemblies in the second and the third concentric rings were ruptured. It corresponds to 55 % of all active zone.

For the verification of the ASTEC calculations, a more detailed investigation of the processes in the single fuel rod with the relative power of 0.98 and the selected accident scenario was provided using TRANSURANUS fuel performance code. This relative power was selected because TRANSURANUS calculation results showed that the margin between burst and equivalent stress is very narrow.

The uncertainty analysis for the TRANSURANUS was performed to ensure that even with uncertainties bound fuel claddings stay intact. The performed analysis demonstrated that fuel assemblies having the relative power of 0.98 will not rupture during the analysed accident, even considering possible uncertainties. Thus, it was concluded that only 232 fuel assemblies will burst. It corresponds to ~ 42 % of the active core (~13 % less compared to the calculations with initial core nodalisation).

Based on TRANSURANUS calculation results, the ASTEC core nodalisation was updated by recalculating the relative power distribution and the number of FAs in each concentric ring. Thermal hydraulic parameters calculated with the updated active core nodalisation showed negligible differences which could be mainly due to the calculation time step and approximations in the code.

Fission product release from the fuel to the coolant, from the coolant to the containment and as well from the containment to the environment was reduced compared to the results obtained with the initial model. Lower activities in the environment (~13 % activity decrease at the 200000 s calculation time from the start of the transient) and in the containment (~18.4 % activity decrease at the 200000 s calculation time from the start of the transient) comparing calculation results of the initial and updated core model were achieved.

Received information on radioactive releases is very important for the further preparation of accident management measures. More precise evaluation of radioactive releases could avoid redundant accident management measures.

CRediT authorship contribution statement

Tadas Kaliatka: Conceptualization, Methodology, Validation, Supervision, Writing – original draft. **Tomas Kačegavičius:** Software, Formal analysis, Investigation. **Algirdas Kaliatka:** Conceptualization, Validation, Writing – review & editing. **Mantas Povilaitis:** Validation, Writing – review & editing. **Andrius Tidikas:** Software, Formal analysis, Investigation, Writing – review & editing. **Andrius Slavickas:** Software, Formal analysis, Investigation.

Declaration of Competing Interest

The authors declare that they have no known competing financial interests or personal relationships that could have appeared to influence the work reported in this paper.

Data availability

Data will be made available on request.

Acknowledgments

This project has received funding from the Euratom research and training programme 2014-2018 under grant agreement No 847656.

References

Ainscough, J.B., Oldfield, B.W., Ware, J.O., 1973. Isothermal grain growth kinetics in sintered UO_2 pellets. J. Nucl. Mater. 49 (2), 117–128.

ANS-5.1 1973 Decay Energy Release Rates Following Shutdown of Uranium-Fueled Thermal Reactors, Draft ANS-5.1 / N18.6, October 1973.

ASTEC V2.1 ISODOP module F. COUSIN, F. JACQ Rapport no PSN-RES/SAG/2015-00366.

ASTEC V2.1 SOPHAEROS module. F. COUSIN Rapport no PSN-RES/SAG/2015-00368.

ASTEC V2.1: Physical modelling of the ICARE module, O. COINDREAU Rapport no PSN-RES/SAG/2016-00422.

L. Chailan et al., "Overview ofASTEC code and models for Evaluation of Severe Accidents in Water Cooled Reactors", Proceedings ofthe IAEA Technical Meeting on Status and Evaluation of Severe Accident Simulation Codesfor Water CooledReactors, Vienna (Austria), October 9-12, (2017).

Chatelard, K. Chevalier-Jabet, J.-P. Van Dorsselaere, H. Nowack, L.E. Herranz, G. Pascal, V.H. Sanchez-Espinoza, The CESAM European project on ASTEC code improvements towards simulation of severe accident management, Int. Workshop on Nuclear Safety and Severe Accident (NUSSA-2014), Sept. 3–5, 2014, Chiba, Japan, 2014.

Chatelard, P., Reinke, N., Arndt, S., Belon, S., Cantrel, L., Carenini, L., et al., 2014b. ASTEC V2 severe accident integral code main features, current V2.0 modelling status, perspectives. Nucl. Eng. Des. 272, 119–135.

https://public.ek-cer.hu/~hozer/CODEX.html, last time accessed 2023-09-11.

Description of the DOSE module of ASTEC V2 L. Cantrel ASTEC-V2/DOC/09-14 Rapport DPAM/SEMIC 2009-357.

Fuel review: fuel design data. Nuclear Engineering International, 42(518), 26-28, 30-31. Anon, 1997.

Ghasabian, M., Mofidnakhaei, F., Talebi, S., 2021. Effect of gap design pressure on the LWR fuel rods lifetime. Kerntechnik 86 (3), 202–209. https://doi.org/10.1515/kern-2021-0004.

Hagen, S., Sepold, L., Hofmann, P., Noack, V., Schanz, G., & Schumacher, G. (1997). The CORA-program: out-of-pile experiments on severe fuel damage. Proceedings of fifth international topical meeting on nuclear thermal hydraulics, operations and safety, (p. 1493). China.

Consideration on the Application of the Safety Requirements for the Design of Nuclear Power Plants, IAEA-TECDOC-1791, 2016.

Kaliatka T., Jusevičiūtė A., Ušpuras E. Adaptation of FEMAXI-6 Code for Fuel Rods of RBMKk-1500 and Employment of Uncertainty and Sensitivity Analysis In: Proceedings of the 17th International Conference on Nuclear Engineering (ICONE17), July 12-16, 2009, Brussels, Belgium.

Kaliatka T., Kačegavičius T., Povilaitis M., Kaliatka A.. Analysis of LOCA accident for BVR-4 under DEC-A conditions using ASTEC code In: *Proceedings of the 10th European Review Meeting on Severe Accidents Research (ERMSAR2022) May 16-19, 2022.* Karlsruhe: Karlsruher Institut für Technologie (KIT), 2022, Log. No. 318, p. 1-11.

Kaliatka, T., Kaliatka, A., Vileiniskis, V., 2016. Application of Best Estimate Approach for Modelling of QUENCH-03 and QUENCH-06 Experiments. Nucl. Eng. Technol. 48 (2), 419–433.

Keisuke OKUMURA, Kensuke KOJIMA, Tsutomu OKAMOTO, Hiroyuki HAGURA, Kenya SUYAM, "Nuclear Data for Severe Accident Analysis and Decommissioning of Nuclear Power Plant", Proceedings of the 2012 Symposium on Nuclear Data, November 15-16, 2012, Research Reactor Institute, Kyoto University, Kumatori, Japan.

Marao, A., Kaliatka, T., Kaliatka, A., Ušpuras, E., 2013. Adaptation of the FEMAXI-6 code and RBMK fuel rods model testing employing the best estimate approach. Kerntechnik Vol. 75, Iss. 3, 72–80. ISSN 0932–3902.

March, P., Simondi-Teisseire, B., 2013. Overview of the facility and experiments performed in Phébus FP. Ann. Nucl. Energy 61, 11–22. https://doi.org/10.1016/j.anucene.2013.03.040. ISSN 0306–4549,.

NUREG-1230 R4, Compendium of ECCS Research for Realistic LOCA Analysis, final report, 1988.

OECD/NEA (2003), Physics of Plutonium Recycling: Volume VII: BWR MOX Benchmark - Specification and Results, Nuclear Science, OECD Publishing, Paris, https://doi.org/10.1787/9789264299054-en.

Official Journal of the European Union (2014), Council Directive 2014/87/EURATOM of 8 July 2014, amending Directive 2009/71/Euratom establishing a Community framework for the nuclear safety of nuclear installations, 72: ISSN 1977-0677, 2014.

Piar and Treogures, 2009L. Piar, N. Treogures ASTEC V2.0: CESAR Physical and Numerical Modeling, Report ASTEC-V2/DOC/09-10 Institut de Radioprotection et de Sûreté Nucléaire (2009).

IAEA Safety Glossary – 2018 Edition, 2019.

SCALE Code System, ORNL/TM-2005/39, Version 6.2.3 (March 2018).

Soti Z., Schubert A., Van Uffelen P., Uncertainty and sensitivity analysis of nuclear fuel performance during aLOCA test case on the basis of the TRANSURANUS code, ANS Best Estimate Plus Uncertainty International Conference (BEPU 2018), Real Collegio, Lucca, Italy, May 13-19, 2018.

J. Stuckert, M. Steinbrueck, M. Grosse: Experimental program QUENCH at KIT on coredegradation during reflooding under LOCA conditions and in the early phase of asevere accident. Proceedings of a Technical Meeting on Modelling of Water CooledFuel Including Design Basis and Severe Accidents, 28 October - 1 November 2013, Chengdu, China.

TEPCO. Information Portal for the Fukushima Daiichi Accident Analysis and Decommissioning Activities, https://fdada.info.

TRANSURANUS handbook, European Commission, Joint Research Centre, 2019 (V1M2J19).

United States Nuclear Regulatory Commission Technical Training Center, "BWR/4 Technology Manual (R-104B)", web page: www.nrc.gov/docs/ML0228/ML022830867.pdf.

M. Vela-Garcia, V. Matuzas, D. Krönung, R. Iglesias, V. Vileiniskis, A. Nieminen, S. Hermsmeyer, N. Reinke, H. Nowack, J. Fontanet, L. Herranz, "Documentation for BWR ASTEC generic input deck" CESAM FP7-GA 323264, 24/02/2017.

S. Wang, H. Muscher, ASTEC-Team at KIT., "Preliminary Analysis of a BWR SBO SA-Sequence with ASTEC2.1rev3". 8th ASTEC Users Club meeting, Aix-en-Provence, F, October 8-11, 2018.

WENRA, Safety Reference Levels for Existing Reactors, WENRA, September 2014. https://www.nrc.gov/docs/ML0230/ML023010606.pdf.